DOI:10.25092/baunfbed. 1692004 *J. BAUN Inst. Sci. Technol., 28(1), 363-374, (2026)*

Waste-to-energy insight: Coupled photocatalytic amoxicillin degradation and hydrogen evolution with NiFe-LDH

Ceren ORAK*

Department of Chemical Engineering, Faculty of Engineering and Natural Sciences, Sivas University of Science and Technology, Sivas, Turkey

Geliş Tarihi (Received Date): 05.05.2025
Kabul Tarihi (Accepted Date):23.08.2025

Abstract

In this study, a nickel–iron layered double hydroxide (NiFe-LDH) photocatalyst was synthesized via a co-precipitation method and applied for the simultaneous degradation of amoxicillin (AMX) and hydrogen (H_2) generation under visible light irradiation. NiFe-LDH was characterized by SEM, FTIR, XRD, and BET analyses, confirming its layered structure, homogeneous elemental distribution, and a specific surface area of 7.56 m^2/g. The photocatalytic performance of NiFe-LDH was systematically evaluated by varying solution pH, catalyst loading, and initial AMX concentration. The optimal AMX degradation (~90%) and hydrogen evolution (58.2 µmol) were achieved at pH 7 with a catalyst loading of 2 g/L and an initial AMX concentration of 5 ppm. Total organic carbon (TOC) and chemical oxygen demand (COD) removal efficiencies reached 65.8% and 84.9%, respectively, under these conditions. The results demonstrate that NiFe-LDH exhibits a promising dual functionality in pollutant mineralization and clean energy production, offering a sustainable waste-to-energy pathway for water treatment applications.

Keywords: *Amoxicillin, hydrogen, NiFe-LDH, photocatalysis, wastewater treatment*

Atıktan enerji üretimine yönelik bir yaklaşım: NiFe-LDH kullanılarak fotokatalitik amoksisilin giderimi ve hidrojen üretiminin birlikte gerçekleştirilmesi

Öz

Bu çalışmada, nikel–demir tabakalı çift hidroksit (NiFe-LDH) fotokatalizörü çöktürme yöntemiyle sentezlenmiş ve görünür ışık altında amoksisilin (AMX) giderimi ile eşzamanlı

* Ceren ORAK, cerenorak@sivas.edu.tr, https://orcid.org/0000-0001-8864-5943

hidrojen (H2) üretimi için kullanılmıştır. NiFe-LDH; SEM, FTIR, XRD ve BET analizleriyle karakterize edilmiş, tabakalı yapısı, homojen element dağılımı ve 7,56 m^2/g özgül yüzey alanına sahip olduğu doğrulanmıştır. NiFe-LDH'nin fotokatalitik performansı, çözeltinin pH'ısı, katalizör yüklemesi ve başlangıç AMX konsantrasyonu değiştirilerek sistematik olarak değerlendirilmiştir. En yüksek AMX giderimi (~%90) ve hidrojen üretimi (58.2 µmol) pH 7, 2 g/L katalizör yüklemesi ve 5 ppm başlangıç AMX konsantrasyonunda elde edilmiştir. Bu koşullarda toplam organik karbon (TOK) ve kimyasal oksijen ihtiyacı (KOİ) giderim verimleri sırasıyla %65.8 ve %84.9 olarak belirlenmiştir. Elde edilen sonuçlar, NiFe-LDH'nin kirletici mineralizasyonu ve temiz enerji üretimi açısından çift işlevli bir potansiyele sahip olduğunu ortaya koymakta ve su arıtım uygulamaları için sürdürülebilir bir atıktan enerjiye dönüşüm yolu sunduğunu göstermektedir.

Anahtar Kelimeler: *Amoksisilin; hidrojen; NiFe-LDH; fotokataliz; atık su arıtımı*

1. Introduction

The widespread use of antibiotics has significantly improved public health outcomes, yet their excessive and often uncontrolled disposal has led to severe environmental challenges [1]. Amoxicillin (AMX), a β-lactam antibiotic commonly prescribed for bacterial infections, is among the most frequently detected pharmaceutical contaminants in aquatic environments [2,3]. Owing to its incomplete degradation in conventional wastewater treatment systems, amoxicillin persists in water bodies, posing risks to aquatic ecosystems and potentially contributing to the emergence of antibiotic-resistant bacteria. These environmental concerns underscore the urgent need for sustainable remediation strategies that not only remove contaminants but also enable value-added resource recovery [4–7].

Among the emerging technologies, advanced oxidation processes (AOPs) -particularly photocatalysis- have attracted growing interest due to their ability to degrade persistent organic pollutants under mild conditions. Beyond pollutant degradation, photocatalytic oxidation has recently been explored for simultaneous hydrogen (H_2) evolution, offering a dual benefit of environmental remediation and clean energy production [8–11]. In these systems, light-activated semiconductor materials generate reactive oxygen species (ROS) and photogenerated electrons, which can drive redox reactions that degrade contaminants and evolve H_2 as concomitant [12–14].

Layered double hydroxides (LDHs), particularly NiFe-LDH, have garnered significant attention as photocatalysts due to their tuneable chemical composition, high surface area, and excellent anion exchange capabilities. The synergistic interaction between Ni^{2+} and Fe^{3+} ions promote visible-light-induced electron–hole pair separation, thereby facilitating the generation of both oxidative radicals and reductive species for H_2 evolution. Moreover, the structural flexibility of LDHs allows for the incorporation of diverse anions, which can further modulate their photocatalytic behaviour for specific applications [15,16].

This study addresses a significant research gap in the field of photocatalytic environmental remediation by integrating the degradation of pharmaceutical pollutants with clean energy recovery. While numerous studies have examined either the

photocatalytic removal of AMX or hydrogen generation separately, only limited research has focused on their simultaneous realization using a single photocatalyst system. Moreover, although NiFe-LDH has been widely studied for water splitting and pollutant degradation due to its visible-light activity and low cost. For instance, Ren et al. used NiFe-LDH@Ni_3S_2 nanosheet arrays as an efficient catalyst for water splitting [17] and Khataee et al. used NiFe-LDH/rGO for the sonophotocatalytic degradation of moxifloxacin (MOX) [18]. In their study, the highest sonophotocatalytic removal efficiency of 90.40% was achieved under optimal conditions: a catalyst loading of 1.0 g/L, MOX concentration of 20 mg/L, ultrasonic power of 150 W, and a natural pH of ~8, with a reaction time of 60 minutes) [18]. The experimental findings revealed that, following an initial adsorption phase and subsequent visible light irradiation for 60 minutes, the addition of H_2O_2 to form a photo-Fenton system enabled tetracycline degradation efficiency to reach as high as 99.11% [19]. However; its dual functionality for both AMX degradation and hydrogen evolution under optimized operational conditions remains largely unexplored. Therefore, this work not only introduces a sustainable strategy for the treatment of antibiotic-laden wastewater but also demonstrates the potential of NiFe-LDH as a multifunctional photocatalyst for waste-to-energy conversion applications.

In this study, NiFe-LDH was synthesized, characterized (SEM-EDX, BET, FTIR, and XRD), and applied for the simultaneous photocatalytic degradation of AMX and H_2 evolution under visible light irradiation. The effects of key operational parameters - including catalyst loading, pH of AMX solution, and initial AMX concentration- were systematically investigated in terms of both degradation efficiency and H_2 evolution. This work contributes to the development of integrated water treatment technologies that facilitate waste-to-energy conversion through the photocatalytic transformation of pharmaceutical pollutants.

2. Material and methods

2.1. Chemicals

Amoxicillin trihydrate (AMX, ≥98%), $Ni(NO_3)_2 \cdot 6H_2O$, $Fe(NO_3)_3 \cdot 9H_2O$, NaOH, HCl and ethanol were purchased from Sigma-Aldrich. All solutions were prepared using deionized water (DW).

2.2. Synthesis of NiFe-LDH

NiFe-LDH was synthesized via a simple co-precipitation method. In a typical synthesis, $Ni(NO_3)_2 \cdot 6H_2O$ and $Fe(NO_3)_3 \cdot 9H_2O$ were dissolved in DW at a molar ratio of 3:1 (Ni:Fe) and the mixture was stirred under a N_2 atmosphere at ambient temperature. NaOH solution (2 N) was then added dropwise to the mixed metal solution to adjust the pH to 10. The resulting suspension was aged at 80°C for 12 h.

2.3. Characterization of NiFe-LDH

The morphology and elemental distribution of NiFe-LDH were characterized by scanning electron microscopy (SEM, QUANTA 400F Field Emission SEM) coupled with energy-dispersive X-ray spectroscopy (EDX). Fourier-transform infrared spectroscopy (FTIR, Shimadzu IRTracer^{TM}-100) was employed to identify surface functional groups within 400–4000 cm^{-1} range. Structural analysis was carried out viaX-ray diffraction (XRD, Philips X'Pert Pro) with Cu Kα radiation (λ = 1.5406 Å). The specific surface area

was measured using Brunauer–Emmett–Teller (BET) analysis (Micromeritics ASAP 2010).

2.4. Experimental study

Photocatalytic degradation experiments were conducted under visible light using a 300 W Xenon lamp. The influence of several parameters-namely pH (3, 5, 7, and 9), initial AMX concentration (5, 10, and 20 ppm), and catalyst loading (1, 2, and 5 g/L)-on the photocatalytic performance was systematically examined. The pH adjustments were carried out using 0.1 M solutions of NaOH and HCl. In a standard test, 0.2 g of NiFe-LDH was dispersed in 100 mL of AMX solution (10 ppm). Then, it was stirred in the dark for 30 min. prior to illumination to ensure adsorption–desorption equilibrium. All experiments were performed in triplicate to ensure reproducibility of the results. Aliquots were taken at specific time intervals during the reaction and analyzed for remaining AMX concentration using a UV-Vis spectrophotometer set at 229 nm. The selection of this detection wavelength was based on previously published studies, which have identified 229 nm as the maximum absorbance for AMX in aqueous solution [20–22]. Alongside AMX degradation, total organic carbon (TOC) removal was assessed with a TOC analyzer (Shimadzu TOC-L), and chemical oxygen demand (COD) was evaluated using COD analysis kits. Additionally, hydrogen gas generated during the photocatalytic reaction was measured by gas chromatography (GC, Agilent 6890) equipped with a thermal conductivity detector. A molecular sieve 5A column was used with N_2 as the carrier gas at a flow rate of 30 mL/min. The GC oven temperature was maintained at 30 °C during the analysis.

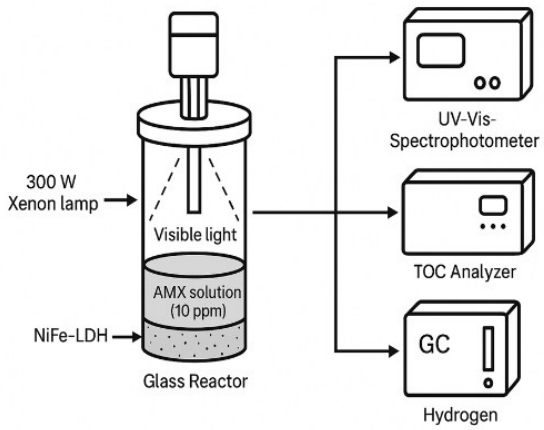

Figure 1. Experimental setup

2.5. Toxicity tests

To assess whether any toxic oxidation by-products were generated during the photocatalytic oxidation process, toxicity experiments were conducted. The evaluation of phytotoxicity was based on root growth inhibition, determined by measuring the root lengths of *Lepidium sativum* seeds exposed to treated and untreated AMX solutions, as well as distilled water. For each condition, 5 mL of the corresponding solution was added to separate Petri dishes containing the seeds. These were then incubated in complete darkness for 72 h. After the incubation period, root lengths were measured, and the inhibition percentage was calculated using the given equation.

$$\text{Root Growth Inhibition (\%)} = \left[\frac{LC - LP}{LC}\right] \text{x}100$$

LC: Average root length of seeds grown in distilled water (control), mm
LP: Average root length of seeds grown in treated or untreated AMX solution, mm

3. Results and discussion

3.1. Characterization Study

The morphology of NiFe-LDH observed via SEM (Figure 2a) revealed plate-like structures typical of LDH materials and similar morphology was previously observed in various reported studies [18,23]. In addition, the EDX mapping (Figure 2b) confirmed the uniform distribution of Ni and Fe throughout the structure, indicating successful synthesis. BET area of Ni-Fe LDH was measured as 7.56 m^2/g. FTIR analysis revealed several distinct features in the spectrum, as shown in Figure 3a. A prominent peak at around 1385 cm^{-1} was observed, which can be attributed to the stretching vibrations of the interlayer nitrate ions in NiFe-LDH. Furthermore, a strong band around 600 cm^{-1} is associated with the Fe–O stretching vibrations in the hydrotalcite structure. The peaks in the range of 400–500 cm^{-1} are related to the O–Ni–O vibration modes [24]. XRD patterns of NiFe-LDH is displayed in Figure 3b and revealed distinct diffraction peaks that correspond to the typical hexagonal structure of LDH. The observed peaks at 11.53°, 22.18°, 32.33°, 34.28°, 38.83°, 45.98°, 60.48°, 65.78°, and 72.08° could be assigned to the (003), (006), (101), (012), (015), (018), (110), (113), (116), and (119) crystallographic planes, respectively. These diffraction peaks align with the well-established pattern for nickel-iron hydrotalcite (JCPDS: 40–0215), confirming the successful formation of the NiFe-LDH phase [17,25]. As a conclusion, the results of characterization analysis were confirmed the successful synthesis of Ni-Fe LDH.

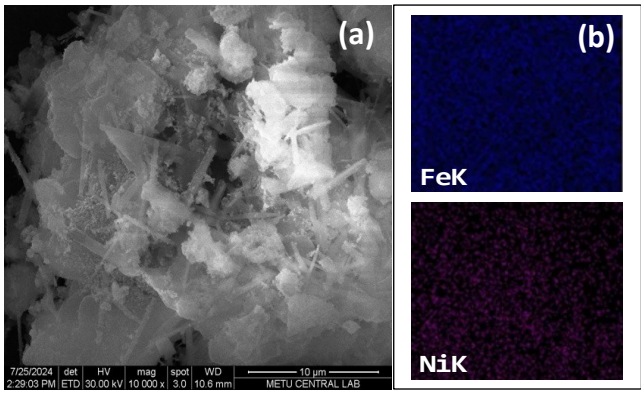

Figure 2. SEM diagram (a) and mapping (b) of NiFe-LDH

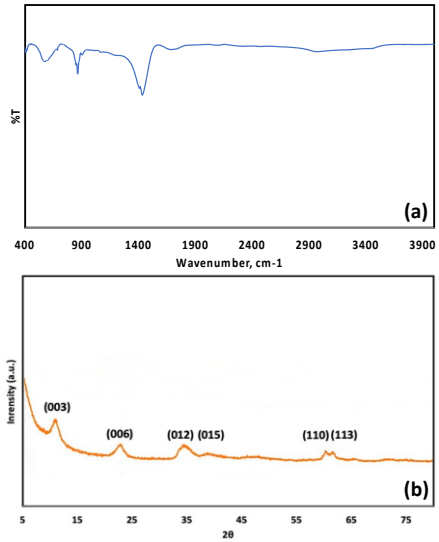

Figure 3. FTIR (a) and XRD (b) spectrum of NiFe-LDH

3.2. Photocatalytic hydrogen evolution from AMX

The photocatalytic degradation of AMX in the presence of NiFe-LDH under visible light irradiation was comprehensively evaluated by systematically investigating the effects of pH, initial AMX concentration, catalyst amount, and the results are given in Figure 4. Figure 5 presents a detailed summary of TOC removal, COD removal, and H_2 evolution over a 2-hour visible light irradiation period are reported under varying experimental conditions, including pH, initial AMX concentration, and NiFe-LDH catalyst loading.

The solution pH significantly influences the photocatalytic degradation process by altering both the surface properties of the photocatalyst and the ionization state of AMX. In the present study, AMX degradation efficiency was investigated at pH 3-9 and it increased with pH up to 7 and then slightly declined at higher pH (pH 9). Lower degradation efficiencies were recorded at acidic and alkaline conditions, due to surface charge interactions and the scavenging of photogenerated charge carriers, which suppress ROS formation. At acidic pH values (3–5), the surface of NiFe-LDH tends to be positively charged, leading to electrostatic repulsion with protonated AMX molecules, thereby reducing adsorption and subsequent degradation, consistent with the literature. Furthermore, excessive H^+ ions may scavenge photogenerated electrons, suppressing ROS formation (•OH, $•O_2^-$) [18,26,27].The highest removal efficiency was observed at pH 7, where almost 75% of AMX was degraded, accompanied by 55.8% TOC and 71.2% COD removal, and 46 μmol of H_2 evolution. This is attributed to: **i.** Minimal electrostatic repulsion, **ii.** Enhanced generation of ROS, **iii.** Favorable adsorption of zwitterionic AMX molecules. Similar observations were reported by Khataee et al., who found that the sonophotocatalytic degradation of moxifloxacin over NiFe-LDH/rGO was optimal near the natural pH (~8), where the catalyst and pollutant interaction was strongest [18]. In contrast, at alkaline pH values (>9), both AMX and the catalyst surface acquire negative charges, leading to electrostatic repulsion and reduced degradation efficiency [18,28,29]. Moreover, hydroxide ions can act as scavengers for photogenerated holes, limiting •OH radical production [16,28]. Thus, near-neutral pH conditions are optimal for achieving maximum photocatalytic degradation of AMX. The influence of catalyst loading was evaluated by varying the NiFe-LDH amount between 1 and 5 g/L (Figure 4b). The degradation efficiency increased with catalyst loading up to 2 g/L, attributed to the availability of more active sites and enhanced photon absorption. However, further increases to 5 g/L led to a decline in AMX degradation and H_2 evolution, likely due to catalyst aggregation and excessive light scattering, which reduced the effective light utilization and decreased ROS generation. The impact of initial AMX concentration on photocatalytic degradation was examined within the range of 5–20 ppm (Figure 4c). In terms of initial AMX concentration, lower AMX concentration (5 ppm) led to the highest AMX degradation (~90%), TOC removal (65.8%), COD removal (84.9%), and hydrogen production (58.2 μmol). This improvement is related to reduced competition for active sites and less light shielding. On the other hand, increasing AMX to 20 ppm resulted in decreased performance due to saturation of catalyst surface and possible inhibition of light penetration. A general trend observed is that higher AMX degradation corresponds to greater TOC/COD removal and H_2 evolution, indicating that the photocatalytic process effectively mineralizes AMX and simultaneously facilitates H_2 production. To better contextualize the performance of the NiFe-LDH photocatalyst, a comparison with literature-reported systems was conducted. Pt/CdS photocatalysts are widely recognized for their high hydrogen evolution rates; for example, Pt/CdS-1h exhibited a specific surface area of 12.03 m^2/g and produced 40.3 μmol/h H_2, while Pt/CdS-3h-S reached 45.1 μmol/h at 13.61 m^2/g [30]. Similarly, noble metal-loaded TiO_2 systems demonstrated

high production capacities: 2 wt% Au–TiO_2 achieved ~550 µmol H_2, 1 wt% Cu–TiO_2 ~420 µmol, and 0.75 wt% Pd–TiO_2 ~300 µmol, with BET surface areas ranging from 50.7 to 100.9 m^2/g [31]. In the present study, the NiFe-LDH catalyst, with a BET surface area of only 7.56 m^2/g, achieved 58.2 µmol H_2 within 2 h (29.1 µmol/h) under visible light, without the use of noble metals, additional oxidants, or co-catalysts. Although the absolute hydrogen production of Pt/CdS and Au/Pd/Cu–TiO_2 systems is higher, these often involve expensive noble metals, more complex synthesis protocols, and, in some cases, UV irradiation. In contrast, the NiFe-LDH system operates effectively under visible light using earth-abundant elements, offering a cost-effective and environmentally friendly approach with the added advantage of simultaneous pollutant degradation and renewable energy generation.

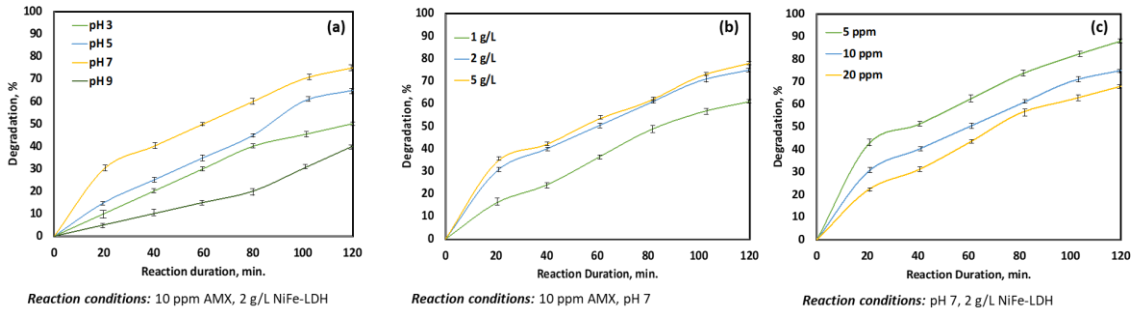

Figure 4. The impact of key reaction parameters: pH (a), catalyst loading (b) and initial AMX concentration (c) on the photocatalytic degradation of AMX

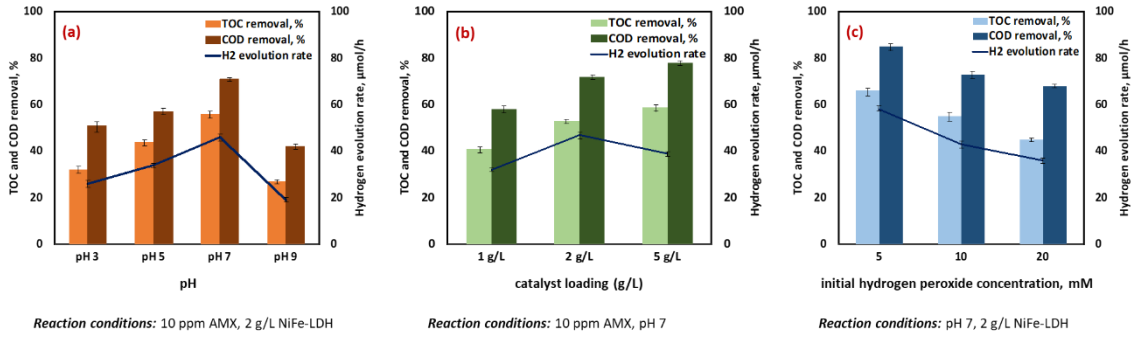

Figure 5. The impact of key reaction parameters: pH (a), catalyst loading (b) and initial AMX concentration (c) on the TOC and COD removal and photocatalytic hydrogen evolution rate.

3.3. Photocatalytic mechanism of NiFe-LDH in AMX Degradation

Upon visible light irradiation, NiFe-LDH absorbs photons, resulting in the excitation of electrons (e^-) from the valence band (VB) to the conduction band (CB), leaving behind positive holes (h^+) in the VB. These photogenerated charge carriers initiate redox reactions at the surface of the catalyst. Specifically, the electrons in the CB reduce dissolved oxygen molecules (O_2) to superoxide radicals ($\bullet O_2^-$), while the holes in the VB oxidize water (H_2O) or hydroxide ions (OH-) to form hydroxyl radicals (•OH) and hydrogen (H_2). Both $\bullet O_2^-$ and •OH are highly reactive oxygen species that attack and degrade the AMX molecules into smaller, less harmful compounds such as CO_2, H_2O, and mineralized by-products, contributing to the overall hydrogen generation. The overall mechanism can be schematically illustrated in Figure 6 and described as follows:

$$NiFe - LDH + h\upsilon \longrightarrow e_{CB}^{-} + h_{VB}^{+}$$
$$e^{-} + O_2 \longrightarrow \bullet O_2^{-}$$
$$h^{+} + H_2O \longrightarrow \bullet OH + H_2$$
$$\bullet OH / \bullet O_2^{-} + AMX \longrightarrow Intermediates \longrightarrow CO_2 + H_2O + H_2$$

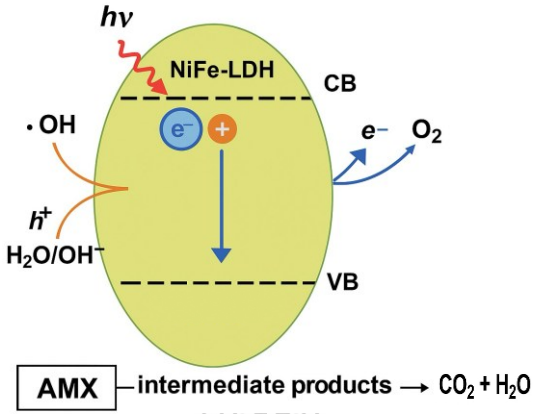

Figure 6. Schematic illustration of the proposed photocatalytic degradation mechanism of AMX using NiFe-LDH under visible light irradiation

3.4.Kinetic study

The kinetic behaviour of the AMX degradation reaction was examined using a first-and second-order rate model. As shown in Figure 7, a plot of $\ln(C_0/C)$ versus reaction time at three different conditions yielded highly linear trends with high R^2 values (R^2=0.99), confirming that the degradation follows the first-order kinetics. The apparent rate constants were calculated from the slopes of the linear regression lines and were found to be 0.0171, 0.0196, and 0.0238 min^{-1} at 25, 35, and 45 °C of reaction temperatures, respectively, suggesting that the reaction rate increases under more favourable reaction conditions. The activation energy (E_a), which was determined to be 13.04 kJ/mol. This relatively low E_a indicates that the reaction proceeds with minimal energy input, which is desirable for energy-efficient applications. Together, these results demonstrate that the reaction exhibits typical first-order kinetics and follows the Arrhenius model, with a low activation barrier supporting its potential for practical implementation under mild operating conditions.

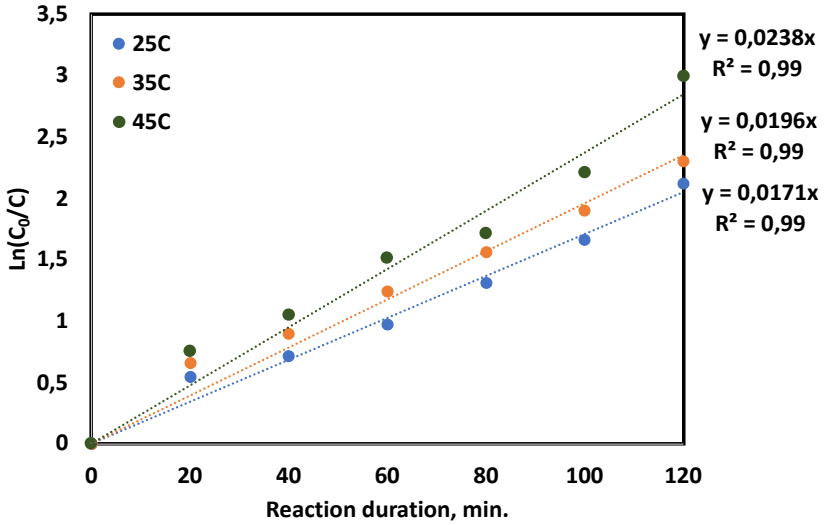

Figure 7. Linearized first-order reaction kinetic

3.5. Toxicity assessment

To evaluate the environmental safety of the photocatalytic degradation process, toxicity tests were conducted under optimal reaction conditions (pH=7, $[AMX]_0$=5 ppm, 2 g/L NiFe-LDH). The potential phytotoxicity of the intermediates and final products formed during the degradation of AMX by NiFe-LDH was examined using *Lepidium sativum* (garden cress) as a bioindicator. The average root elongation of seedlings exposed to the treated AMX solution was measured as 22.65 mm, compared to 18.27 mm for those grown in untreated AMX solution and 39.12 mm for those grown in distilled water. Untreated AMX solution caused significant growth inhibition in the roots, whereas the roots treated with the photocatalytically degraded solution showed a noticeable increase in length. The growth inhibition percentages were calculated as 42.1% and 53.3% for treated and untreated AMX solutions, respectively, indicating a reduction in phytotoxicity after treatment. These findings suggest that the NiFe-LDH does not only effectively degrades the AMX but also reduces the toxicity of the resulting solution, enhancing its potential for practical environmental applications.

As a conclusion, the NiFe-LDH photocatalyst synthesized in this study demonstrated strong efficiency in degrading AMX, achieving 88% removal under optimized conditions. This result is on par with, or even superior to, many photocatalysts previously reported for similar antibiotic compounds, particularly tetracycline. For instance, degradation rates of 90% and 83.1% were reported for TiO_2/NiAl-LDH [32] and Ag_3VO_4/ZnTi-LDH [33], respectively, while LDH-Ag_2O/Ag [34] and MgAl-LDH/$(BiO)_2CO_3$ [35] were achieved slightly higher values of 92% and 97.2%. Although some photocatalysts with enhanced activity, such as NiFe LDH/$Bi_4O_5I_2$ [36] and $Cu_{2.5}Ni_{0.5}$Co-LDH/GO [37], exhibited degradation efficiencies exceeding 95% via photo-Fenton or hybrid pathways, these typically involve more elaborate setups and additional reagents. In contrast, this work employs NiFe-LDH catalyst activated under visible light, without the need for added oxidants or co-catalysts, offering a more straightforward and eco-friendly solution with competitive performance. Furthermore, the toxicity evaluation showed a noticeable decrease in phytotoxicity following treatment, supporting the environmental safety of the approach. In summary, the findings highlight NiFe-LDH as an effective and sustainable photocatalyst for AMX removal from wastewater streams.

Conclusion

This study demonstrated the successful synthesis of NiFe-LDH via a simple co-precipitation method and its efficient application in the simultaneous photocatalytic degradation of AMX and H_2 production under visible light. Structural and morphological analyses confirmed the formation of a layered double hydroxide with uniform Ni and Fe distribution and characteristic functional groups. Photocatalytic experiments revealed that near-neutral pH (pH 7), moderate catalyst loading (2 g/L), and lower AMX concentration (5 ppm) provided optimal conditions for AMX, TOC and COD removal and H_2 evolution. The correlation between AMX degradation, TOC/COD reduction, and hydrogen generation highlights the effectiveness of the NiFe-LDH photocatalyst in facilitating both environmental remediation and renewable energy conversion. The results suggest that NiFe-LDH has potential for dual-function photocatalytic applications in wastewater treatment and energy recovery.

References

[1] Orak, C. Application of response surface methodology for bioenergy generation in a yeast-based microbial fuel cell. **RSC Advances, 14,** 34356–61, (2024).

[2] Mirzaei, A., Chen, Z., Haghighat, F., Yerushalmi, L. Magnetic fluorinated mesoporous g-C_3N_4 for photocatalytic degradation of amoxicillin: Transformation mechanism and toxicity assessment. **Applied Catalysis B: Environmental, 242,** 337–48, (2019).

[3] Verma M, Haritash AK. Photocatalytic degradation of Amoxicillin in pharmaceutical wastewater: A potential tool to manage residual antibiotics. **Environmental Technology & Innovation, 20,** 101072, (2020).

[4] Dou, M., Wang, J., Gao, B., Xu, C., Yang, F. Photocatalytic difference of amoxicillin and cefotaxime under visible light by mesoporous g-C_3N_4: Mechanism, degradation pathway and DFT calculation. **Chemical Engineering Journal, 383,** 123134, (2020).

[5] Kanakaraju, D., Kockler, J., Motti, C.A., Glass, B.D., Oelgemöller, M. Titanium dioxide/zeolite integrated photocatalytic adsorbents for the degradation of amoxicillin. **Applied Catalysis B: Environmental, 166–167,** 45–55, (2015).

[6] Orak, C, Öcal, B, Yüksel, A. Treatment of Sugar Industry Wastewater by Using Subcritical Water as a Reaction Media. **ChemistrySelect, 8,** e202203300, (2023).

[7] Hansu, TA, Kaya, Ş, Çağlar, A, Akdemir, M, Kivrak, HD, Orak, C, Horoz, S, Kaya, M. Enhanced catalytic performance of Pd/PMAc-g-CNT composite for water splitting and supercapacitor applications. **Ionics, 30**, 5513–5524, (2024).

[8] Orak, C. Enhanced degradation of Procion Red MX-5B using Fe-doped corn cob ash and Fe-doped g-C_3N_4. **Energy Sources, Part A: Recovery, Utilization, and Environmental Effects, 46,**14244–58, (2024).

[9] Orak, C. Treatment of sugar industry wastewater via Fenton oxidation with zero-valent iron. **Cumhuriyet Science Journal, 45,** 100–4, (2024).

[10] Orak, C., Oğuz, T., Horoz, S. Facile synthesis of Mn-doped CdS nanoparticles on carbon quantum dots: towards efficient photocatalysis. **Journal of the Australian Ceramic Society, 60,** 1657-1667, (2024).

[11] Haste, Z.Ö., Horoz, S., Orak, C., Biçer, E. Green-synthesized SnO_2 derived from Kombucha tea and assessment of its photocatalytic activity for the degradation of Procion Red MX-5B. **ChemistrySelect, 9 (43),** e202403264, (2024).

[12] Bakır, R., Orak, C. Stacked machine learning approach for predicting evolved hydrogen from sugar industry wastewater. **International Journal of Hydrogen Energy 85,** 75–87, (2024).

[13] Bakır, R., Orak, C., Yüksel, A. A machine learning ensemble approach for predicting solar-sensitive hybrid photocatalysts on hydrogen evolution. **Physica Scripta, 99,** 076015, (2024).

[14] Arabacı, B., Bakır, R., Orak, C., Yüksel, A. Predictive modeling of photocatalytic hydrogen production: Integrating experimental insights with machine learning on Fe/g-C_3N_4 catalysts. **Industrial & Engineering Chemistry Research, 64,** 5184–5199, (2025).

[15] Jabeen, A., Salem Alsaiari, N., MohammedSaleh Katubi, K., Shakir, I., Alrowaili, Z.A., Al-Buraihi, M.S., Warsi, M.F. Synthesis and characterisation of MXene based-LDH photocatalytic materials for the removal of toxic pharmaceutical effluents. **Journal of Molecular Liquids, 405,** 125066, (2024).

[16] Chen, Y., Haihua, X., Khan, M.S., Shiqi, H., and Zhu, S. Recent advances in layered double hydroxides for pharmaceutical wastewater treatment: A critical

review. **Critical Reviews in Environmental Science and Technology,** 1-27, (2025).

[17] Ren, L., Wang, C., Li, W., Dong, R., Sun, H., Liu, N., et al. Heterostructural NiFe-LDH@Ni_3S_2 nanosheet arrays as an efficient electrocatalyst for overall water splitting. **Electrochimica Acta, 318,** 42–50, (2019).

[18] Khataee, A., Rad, T.S., Nikzat, S., Hassani, A., Aslan, M.H., Kobya, M., Demirbaş, E. Fabrication of NiFe layered double hydroxide/reduced graphene oxide (NiFe-LDH/rGO) nanocomposite with enhanced sonophotocatalytic activity for the degradation of moxifloxacin. **Chemical Engineering Journal, 375,** 122102, (2019).

[19] Liu, X., Zhou, Y., Sun, S., Bao, S. Study on the behavior and mechanism of NiFe-LDHs used for the degradation of tetracycline in the photo-Fenton process. **RSC Advances, 13**, 31528–31540, (2023).

[20] Keşir, M.K., Sökmen, M., Bıyıklıoğlu, Z. Photocatalytic efficiency of metallo phthalocyanine sensitized TiO_2 (MPc/TiO_2) nanocomposites for Cr(VI) and antibiotic amoxicillin. **Water, 13**, 2174, (2021).

[21] Ataklti, A., Alemu, K., Abebe, B. Study of the self-association of amoxicillin, thiamine and the hetero-association with biologically active compound chlorogenic acid. **African Journal of Pharmacy and Pharmacology, 10**, 393–402, (2016).

[22] Hrioua, A., Aghris, S., Ajermoun, N., Ettadili, F., Farahi, A., Lahrich, S., et al. Electrochemical investigation of amoxicillin interaction with some metal ions related to complexation process. **Journal of The Electrochemical Society, 167**, 126501, (2020).

[23] Li, X., Hao, X., Wang, Z., Abudula, A., Guan, G. In-situ intercalation of NiFe LDH materials: An efficient approach to improve electrocatalytic activity and stability for water splitting. **Journal of Power Sources, 347,** 193–200, (2017).

[24] Tian, M., Liu, C., Neale, Z.G., Zheng, J., Long, D., Cao, G. Chemically Bonding NiFe-LDH Nanosheets on rGO for Superior Lithium-Ion Capacitors. **ACS Applied Materials & Interfaces, 11,** 35977–86, (2019).

[25] Sirisomboonchai, S., Li, S., Yoshida, A., Li, X., Samart, C., Abudula, A., Guan, G. Fabrication of NiO Microflake@NiFe-LDH Nanosheet Heterostructure Electrocatalysts for Oxygen Evolution Reaction. **ACS Sustainable Chemistry & Engineering, 7,** 2327–34, (2019).

[26] Qutob, M., Shakeel, F., Alam, P., Alshehri, S., Ghoneim, M.M., Rafatullah, M. A review of radical and non-radical degradation of amoxicillin by using different oxidation process systems. **Environmental Research, 214,** 113833, 2022.

[27] Elmolla, E.S., Chaudhuri, M. Photocatalytic degradation of amoxicillin, ampicillin and cloxacillin antibiotics in aqueous solution using UV/TiO_2 and UV/H_2O_2/TiO_2 photocatalysis. **Desalination, 252,** 46–52, (2010).

[28] Sun, C., Wang, Y., Jiang, B., Hu, S., Wang, Y., Zhang, C., Li, G. Self-catalyst degradation of amoxicillin in alkaline condition driven by superoxide radical. **Chemical Engineering Journal, 477,** 146942, (2023).

[29] Tran, M.L., Fu, C.C., Juang, R.S. Removal of metronidazole and amoxicillin mixtures by UV/TiO_2 photocatalysis: an insight into degradation pathways and performance improvement. **Environmental Science and Pollution Research, 26,** 11846–55, (2019).

[30] Li, Y., Du, J., Peng, S., Xie, D., Lu, G., Li, S. Enhancement of photocatalytic activity of cadmium sulfide for hydrogen evolution by photoetching. **International Journal of Hydrogen Energy, 33**, 2007–2013, (2008).

[31] Sreethawong, T., Yoshikawa, S. Comparative investigation on photocatalytic hydrogen evolution over Cu-, Pd-, and Au-loaded mesoporous TiO_2 photocatalysts. **Catalysis Communications, 6**, 661–668, (2005).

[32] Shao, L., Cheng, S., Yang, Z., Xia, X., Liu, Y. Nickel aluminum layered double hydroxide nanosheets grown on oxygen vacancy-rich TiO_2 nanobelts for enhanced photodegradation of an antibiotic. **Journal of Photochemistry and Photobiology A: Chemistry, 411,** 113209, (2021).

[33] Xiong, J., Zeng, H.Y., Chen, C.R., Li, S., Xu, S., An, D.S. Ag_3VO_4 anchored ZnTi hydrotalcite microspheres with rosette-like structure for tetracycline degradation. **Applied Clay Science, 208,** 106118, (2021).

[34] Chen, C.R., Zeng, H.Y., Yi, M.Y., Xiao, G.F., Zhu, R.L., Cao, X.J., Shen, S.G., Peng, J.W. Fabrication of Ag_2O/Ag decorated ZnAl-layered double hydroxide with enhanced visible light photocatalytic activity for tetracycline degradation. **Ecotoxicology and Environmental Safety, 172,** 423–431, (2019).

[35] Sun, C., Wang, Y., Wu, L., Hu, J., Long, X., Wu, H., Jiao, F. In situ preparation of novel p–n junction photocatalyst MgAl-LDH/$(BiO)_2CO_3$ for enhanced photocatalytic degradation of tetracycline. **Materials Science Semiconductor Processing, 150,** 106939, (2022).

[36] Zhu, C., Wang, Y., Qiu, L., Yang, W., Yu, Y., Li, J., Liu, Y. Z-scheme NiFe LDH/$Bi_4O_5I_2$ heterojunction for photo-Fenton oxidation of tetracycline. **Journal of Alloys and Compdounds, 944,** 169124, (2023).

[37] Wu, Z., Gu, Y., Xin, S., Lu, L., Huang, Z., Li, M., Cui, Y., Fu, R., Wang, S. Cu_xNi_yCo-LDH nanosheets on graphene oxide: an efficient and stable Fenton-like catalyst for dual-mechanism degradation of tetracycline. **Chemical Engineering Journal, 434,** 134574, (2022).